Available online at www.sciencedirect.com
ScienceDirect
Journal of Luminescence 128 (2008) 190–198
JOURNAL OF LUMINESCENCE
www.elsevier.com/locate/jlumin

Evaluation of intramolecular energy transfer process in the lanthanide(III) *bis*- and *tris*-(TTA) complexes: Photoluminescent and triboluminescent behavior

Ercules E.S. Teotonio[a,*], Gerson M. Fett[b], Hermi F. Brito[b], Wagner M. Faustino[c], Gilberto F. de Sá[d], Maria Cláudia F.C. Felinto[e], Regina H.A. Santos[f]

[a]*Departamento de Química, Universidade Federal de Goiás, Campus Catalão, CEP 75704-020 Catalão, GO, Brazil*
[b]*Departamento de Química Fundamental, Instituto de Química da Universidade de São Paulo, CEP 05508-900, São Paulo, SP, Brazil*
[c]*Departamento de Eletrônica Quântica, Instituto de Física Gleb, Universidade Estadual de Campinas, Cidade Universitária, CEP 13083-970, Campinas, SP, Brazil*
[d]*Departamento de Química Fundamental, Universidade Federal de Pernambuco, Cidade Universitária, CEP 50670-910, Recife, PE, Brazil*
[e]*Instituto de Pesquisas Energéticas e Nucleares Travessa R 400 Cidade Universitária, CEP 05508-970, São Paulo, SP, Brazil*
[f]*Instituto de Química de São Carlos, USP, C.P. 780, CEP 13560-970, São Carlos, SP, Brazil*

Received 29 January 2007; received in revised form 9 July 2007; accepted 11 July 2007
Available online 20 July 2007

Abstract

This work reports the energy transfer mechanism process of $[Eu(TTA)_2(NO_3)(TPPO)_2]$ (*bis*-TTA complex) and $[Eu(TTA)_3(TPPO)_2]$ (*tris*-TTA complex) based on experimental and theoretical spectroscopic properties, where TTA = 2-thienoyltrifluoroacetone and TPPO = triphenylphosphine oxide. These complexes were synthesized and characterized by elemental analyses, infrared spectroscopy and thermogravimetric analysis. The theoretical complexes geometry data by using Sparkle model for the calculation of lanthanide complexes (SMLC) is in agreement with the crystalline structure determined by single-crystal X-ray diffraction analysis. The emission spectra for $[Gd(TTA)_3(TPPO)_2]$ and $[Gd(TTA)_2(NO_3)(TPPO)_2]$ complexes are associated to $T \rightarrow S_0$ transitions centered on coordinated TTA ligands. Experimental luminescent properties of the *bis*-TTA complex have been quantified through emission intensity parameters Ω_λ ($\lambda = 2$ and 4), spontaneous emission rates (A_{rad}), luminescence lifetime (τ), emission quantum efficiency (η) and emission quantum yield (q), which were compared with those for *tris*-TTA complex. The experimental data showed that the intensity parameter value for *bis*-TTA complex is twice smaller than the one for *tris*-TTA complex, indicating the less polarizable chemical environment in the system containing nitrate ion. A good agreement between the theoretical and experimental quantum yields for both Eu(III) complexes was obtained. The triboluminescence (TL) of the $[Eu(TTA)_2(NO_3)(TPPO)_2]$ complexes are discussed in terms of ligand-to-metal energy transfer.
© 2007 Elsevier B.V. All rights reserved.

Keywords: Lanthanide ions; β-diketonate; Complexes; Photo and Triboluminescence

1. Introduction

β-Diketonates is one of the most studied ligands of trivalent lanthanide complexes. This is probably owing to the higher ability of β-diketonate organic ligands to act as luminescence sensitizers for Ln(III) ions and also due to the higher thermodynamic stability presented by their complexes. The luminescence properties exhibited by Ln(III)–β-diketonate complexes make it possible to use them in numerous applications, ranging from diagnostic probes in clinical analyses to emitter layers in light-emitting diodes (LEDs) [1–9]. These complexes have also attracted much interest within theoretical chemistry, and have become target of intensive studies in the investigation of intramolecular energy-transfer processes from ligands to Ln(III) ion, and theoretical models used to describe geometric and spectroscopic properties of lanthanide coordination compounds [1,10–12]. It is also important to mention that although some lanthanide β-diketonates

*Corresponding author. Tel.: +55 64 3441 1503; fax: +55 64 3441 1515.
E-mail address: ercules@catalao.ufg.br (E.E.S. Teotonio).

0022-2313/$ - see front matter © 2007 Elsevier B.V. All rights reserved.
doi:10.1016/j.jlumin.2007.07.005

presented photodecomposition under UV irradiation in the solution or in the thin film, one strategy to decrease this effect generally used is the incorporation of β-diketonate complexes in polymers and organic/inorganic hybrids [13–16].

Among Ln(III)–β-diketonate complexes tetrakis(M[Ln(β-diketonate)$_4$]), where M is a monovalent cation such as an alkali-metal ions, quaternary ammonium ions or a protonated organic base (pyridinium, piperidinium, isoquinolinium, etc.) and *tris*-compounds of formula [Ln(β-diketonate)$_3$L$_n$] are the most extensively investigated [3]. L is additional neutral ligands that coordinate to lanthanide center to replace the solvent and water molecules that may act as luminescent quencher, where these ligands are sulfoxides, phosphine oxides, amides and heteroaromatics, etc. [1].

In contrast to *tris* and tetrakis(β-diketonate) complexes of Ln(III) ions, the synthesis and spectroscopic investigation of *bis*-β-diketonate compounds are rarely reported in literature. The latter are generally synthesized in special conditions, such as acid media, and also when the neutral ligands contain bulky substituent groups. The main examples of these compounds were synthesized by Bünzli and Fu and they present tributylphosphine oxide (TBPO) and triphenylphosphine oxide (TPPO) as neutral ligands, respectively [17,18].

Many Ln compounds also present triboluminescent (TL) properties, although until now the mechanism by which this phenomenon occurs is not yet completely understood [3]. In Eu(III) complexes, TL is expected to be caused by the fracturing process through an intermediate excitation of ligand [19–21]. However, to the best of our knowledge, up to now there is no work reporting experimental support for this process, such as TL spectra of the similar Gd^{3+}-complexes in which only emission from ligand is detected, confirming the ligand excitation and ligand-to-Eu(III) energy transfer processes.

In this paper, we report spectroscopic measurements that permit a detailed analysis of the photoluminescent (PL) and TL processes of Eu(III)–TTA complexes. In addition, the comparative study of structural and PL properties between *bis*- and *tris*-TTA complexes is also presented. Photophysical properties of these compounds are discussed based on experimental data of the Ω_2 and Ω_4 intensity parameters, radiative (A_{rad}) and non-radiative decay rates (A_{nrad}), quantum emission efficiency (η) and quantum yield (q). Theoretical analysis of the geometries and the intramolecular ligand-to-Eu(III) energy transfer for the [Eu(TTA)$_2$(NO$_3$)(TPPO)$_2$] and [Eu(TTA)$_3$(TPPO)$_2$] complexes are also reported.

2. Experimental

2.1. Synthesis of the [Ln(TTA)$_2$(NO$_3$)(TPPO)$_2$] complexes

Methanol, thenoyltrifluoroacetonate and TPPO reagents were purchased from Aldrich Co. and used as received. All chemicals and solvents used in the syntheses of the Ln(III)-complexes were of analytical grade and used without additional purification.

For a solution containing 3 equiv. of HTTA (1.00 g, 6.7×10^{-3} mol) and 2 equiv. of TPPO in 40 mL of methanol was added by dropping (under stirring) 1 equiv. of $Ln(NO_3)_3\cdot6H_2O$ (0.61 g, 1.7×10^{-3} mol) in 10 mL of methanol. The resultant solution was in standby for 2 days, forming white crystals, which were filtered, washed with cooled methanol to remove the excess of ligand and dried in vacuum desiccator, with 80% yielding of the [Ln(TTA)$_2$(NO$_3$)(TPPO)$_2$] complex. However, the *tris*-TTA complex was synthesized as described by Silva [22].

2.2. Apparatus

Elemental analyses of carbon, hydrogen and nitrogen of the complexes were performed on a Perkin-Elmer model 240 microanalyzer. The Ln(III) ion contents were performed by complexometric titration with disodium ethylenediaminetetraacetic acid (EDTA) salt [23]. Infrared spectra were recorded in KBr pellets on a Bomen model MB-102 spectrophotometer in the range 4000–400 cm^{-1}. Thermogravimetric analyses (TGA) were performed on a thermobalance Schimadzu TGA-50. The samples were placed in platinum containers, and the TG curves were recorded in dynamic nitrogen atmosphere of 50 cm^3 min^{-1} under a heating rate of 10 °C min^{-1} from room temperature up to 900 °C.

Steady-state excitation and emission spectra at room (~298 K) and liquid nitrogen temperatures were recorded at an angle of 22.5° (front face) with a spectrofluorimeter (SPEX-Fluorolog 2) with double grating 0.22 m monochromator (SPEX 1680), and a 450 W Xenon lamp as excitation source. All spectra were recorded using a detector mode correction. The luminescence decay curves of the emitting levels were measured using a phosphorimeter SPEX 1934D accessory coupled to the spectrofluorometer.

TL spectra of the complexes were measured by fracturing the crystals with a glass stirring rod in a darkroom and the luminescent spectra were recorded using a plug-in high-sensitivity fiber-optical UV–vis shortwave master spectrometer, fitted with a grating blazed at 500 nm with 600 grooves per millimeter, with a 2048-element linear CCD-array detector (PC, 2000, Ocean Optics, Inc.).

3. Results and discussion

3.1. Characterization of the [RE(TTA)$_2$(NO$_3$)(TPPO)$_2$] complexes

3.1.1. Elemental analysis

The elemental analyses of CHN, and the complexometric titration with disodium ethylenediaminetetraacetic acid (EDTA) salt confirm the general formula [RE(TTA)$_2$(NO$_3$)(TPPO)$_2$] for the complexes. Anal. Calc. for

$[Eu(TTA)_2(NO_3)(TPPO)_2]$: Eu^{3+}, 12.53; C, 51.49; H, 3.16; N, 1.15 and found: Eu^{3+}, 12.46; C, 51.48; H, 3.21; N, 1.21. IR (KBr, cm^{-1}): 3064 (w), 1610 (s), 1574 (m), 1538 (s), 1502 (s), 1470 (s), 1442 (m), 1418 (s), 1381 (w), 1357 (m), 1305 (s), 1240 (m), 1180 (s), 1136 (s), 1063 (m), 934 (w), 785 (m), 725 (s), 697 (m), 645 (w). Anal. Calc. for $[Gd(TTA)_2(NO_3)(TPPO)_2]$: Gd^{3+}, 12.91; C, 51.27; H, 3.14; N, 1.15 and found: Gd^{3+}, 12.83; C, 51.32; H, 3.20; N, 1.10. IR (KBr, cm^{-1}): 3062 (w), 1610 (s), 1577 (m), 1542 (s), 1500 (s), 1471 (s), 1447 (m), 1418 (s), 1377 (w), 1357 (m), 1307 (s), 1240 (m), 1182 (s), 1135 (s), 1063 (m), 935 (w), 781 (m), 722 (s), 701 (m), 646 (w).

3.1.2. Infrared spectroscopy

Infrared spectra of Eu(III) and Gd(III) complexes exhibit no broad band in the spectral range 4500–4300 cm^{-1} due the O–H stretching vibration of water molecule, indicating that these compounds are anhydrous. This result is different from that reported by Fu et al. for *bis*-TTA complex, which was obtained in monohydrated form [18]. IR spectra also show two strong bands at 1688 and 1557 cm^{-1} attributed to $\nu_s(C{=}O)$ and $\nu_{as}(C{=}O)$ vibrational modes of TTA ligand that are in concordance with TTA acting as chelate ligand. By comparing the IR spectra of the free TPPO ligand (non-coordinate) and those of the complexes, a shift of stretching frequency P=O from 1200 cm^{-1} to around 1180 cm^{-1} is revealed, indicating the coordination of TPPO to lanthanide ions via oxygen atom.

The NO_3^- group may act as monodentate or bidentate ligand to metal ion, or may still act as a non-coordinated ionic group [24–26]. The type of nitrate group presented in the complexes is generally investigated considering the combination band ($\nu_1+\nu_4$), which appears in the spectral range 1700–1800 cm^{-1}, and those broad bands around 1300–1500 cm^{-1}. In the first case, the splitting parameter ($\Delta\nu$) is equal to ~30 cm^{-1}, indicating the bidentate coordination mode of the NO_3 ligand. These spectral data are reinforced by presence of two bands around 1180 and 1136 cm^{-1} assigned to the NO_3^- group presenting the C_{2v} symmetry upon coordination to the Ln(III) ions.

3.1.3. Thermogravimetric analysis

Fig. 1 shows the TG curves for both Eu^{3+} and Gd^{3+}-complexes in the temperature interval 25–900 °C. As it can be seen, the curves exhibit similar profiles and there is no weight loss up to 230 °C, confirming the anhydrous character of complexes obtained by CHN% elemental analysis. These results are in accordance to that for samarium compound of stoichiometric formula $[Sm(TTA)_2(TPPO)_2(NO_3)]$ reported by Fu et al. [18].

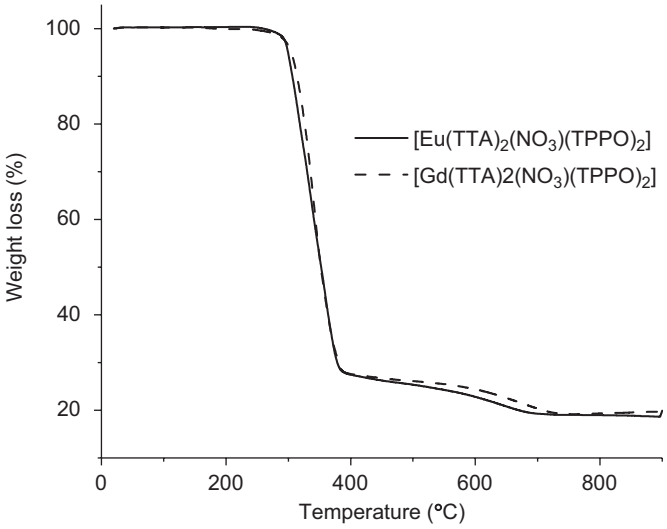


Fig. 1. Thermogravimetric curves of the $Eu(TTA)_2(NO_3)$ $(TPPO)_2]$ and $[Gd(TTA)_2(NO_3)(TPPO)_2]$ complexes.

3.2. Photoluminescence investigations

In order to determine the energetic positions of the singlet (S) and triplet (T) states arising from TTA ligand in the *bis*- and *tris*-TTA complexes, the emission spectra for similar Gd(III)-complexes were recorded at 77 K. It is important to mention that in view of the fact that the Gd(III) ion excited states have energies much higher than TTA excited states, the ligand-to-metal energy transfer processes are disable. Thus, generally, the emission spectra of Gd^{3+}-coordination compounds display only characteristic broad bands arising from the S and T states of TTA ligand [1,6]. This behavior is illustrated by the emission spectra for Gd^{3+}–TTA complexes presented in Fig. 2. An examination of the emission spectrum for Gd(III) *tris*-TTA complex revealed a similar spectral profile of the $[Gd(TTA)_2(NO_3)(TPPO)_2]$, showing broad bands with maxima around 500 nm. The higher values of the lifetime of the $[Gd(TTA)_2(NO_3)(TPPO)_2]$ (3.074 ms) and $[Gd(TTA)_3(TPPO)_2]$ (3.278 ms) complexes, recorded at liquid nitrogen temperature, indicate that these bands are associated to $T\rightarrow S_0$ transitions centered on coordinated TTA ligands. However, the emission band of the $[Gd(TTA)_2(NO_3)(TPPO)_2]$ is shifted to higher energy as compared to the one in the $[Gd(TTA)_3(TPPO)_2]$ compound. This result may be a consequence of the shorter ligand–Gd^{3+} ion distances in the former.

The energy values of TTA triplet states were estimated from the shortest wavelength on the base of the emission bands, which correspond to the $T\rightarrow S_0$ transitions (0–0 phonon), whereas, the excited S states were taken as the longest wavelength from the absorption spectra corresponding to the $S_0\rightarrow S$ transition (0–0 phonon). The experimental excited S and T states of TTA ligand for the $[Eu(TTA)_2(NO_3)(TPPO)_2]$ and $[Eu(TTA)_3(TPPO)_2]$ complexes are ($S = 26702\,cm^{-1}$ and $T = 21645\,cm^{-1}$) for the former and ($S = 24975\,cm^{-1}$ and $T = 20661\,cm^{-1}$) for the latter.

Excitation and emission spectra of the $[Eu(TTA)_2(NO_3)(TPPO)_2]$ recorded at 77 K are given in Fig. 3. The excitation spectrum recorded in the range 250–590 nm,

under emission on $^5D_0 \rightarrow {}^7F_2$ hypersensitive transition at 615 nm (Fig. 3a), is dominated by two overlapped broad bands corresponding to $S_0 \rightarrow S_1$ absorption of the TTA ligands. These optical data give evidence that Eu(III) ion luminescence is sensitized by TTA via *antenna* effect. In this effect the aromatic chromophore (sensitizer) absorbs energy that is then transferred towards the lanthanide cation, which in its turn emits light [6–8,17].

In Fig. 3a, $[Eu(TTA)_2(NO_3)(TPPO)_2]$ exhibits similar spectral profile compared to the *tris*-TTA complex [18,22], suggesting the lesser steric hindrance presented in the *bis*-TTA complex, which decrease the metal–donor atoms distances, and has only a moderate effect on the S states of the ligand. Excitation spectrum also displays narrow bands assigned to $^7F_0 \rightarrow {}^{2S+1}L_J$ transitions to Eu(III) ion, such as $^7F_0 \rightarrow {}^5G_6$ (361 nm), $^7F_0 \rightarrow {}^5H_4$ (374 nm), $^7F_0 \rightarrow {}^5L_6$ (394 nm), $^7F_0 \rightarrow {}^5D_2$ (464 nm), $^7F_0 \rightarrow {}^5D_1$ (532 nm) and $^7F_0 \rightarrow {}^5D_0$ (578 nm). However, these peaks are less intense than those broad bands because of the low molar absorption coefficient of the lanthanide ions and due to the operative *antenna* effect in the Eu–TTA complexes.

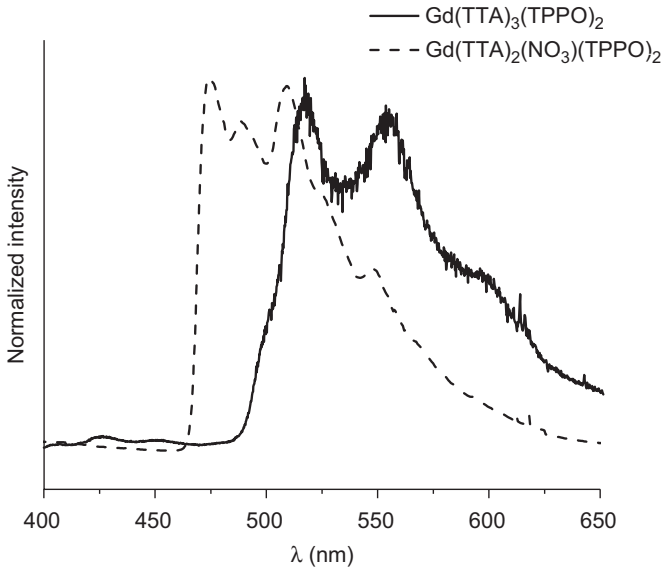


Fig. 2. Emission spectra of the $[Gd(TTA)_2(NO_3)(TPPO)_2]$ and $[Gd(TTA)_3(TPPO)_2]$ complexes in solid state, at 77 K, under excitation at 350 nm.

Fig. 3b shows the emission spectrum of the $[Eu(TTA)_2(NO_3)(TPPO)_2]$ complex under excitation at 350 nm, at 77 K. This spectrum consists of typical narrow bands of central Eu(III) ion assigned to $^5D_0 \rightarrow {}^7F_J$ transitions ($J = 0$, 1, 2, 3 and 4), presenting hypersensitive $^5D_0 \rightarrow {}^7F_2$ transition (~617 nm) as the most prominent. The emission spectrum of $[Eu(TTA)_2(NO_3)(TPPO)_2]$ complex in the spectral range of 580–630 nm, at 300 K, has been reported recently by Bukvetskii et al. [24]. In that paper, the authors attributed some Stark-components of the $^5D_0 \rightarrow {}^7F_2$ transition to the $^5D_0 \rightarrow {}^7F_1$ and $^5D_0 \rightarrow {}^7F_3$ transitions. Thus, Fig. 3b presents new assignment of $^5D_0 \rightarrow {}^7F_J$ transitions centered on Eu^{3+} ion.

Several less intense bands are observed in all spectral range from 500 to 720 nm that are assigned to the following transitions: $^5D_1 \rightarrow {}^7F_0$ (526.4 nm), $^5D_1 \rightarrow {}^7F_1$ (536.4 and 537.6 nm), $^5D_1 \rightarrow {}^7F_2$ (552.6 nm) and $^5D_1 \rightarrow {}^7F_3$ (584 nm). A significant number of vibronic transitions much less intense is also observed in the emission spectrum. The absence of broad bands arising from the ligand centered transitions indicates that there is an efficient intramolecular energy transfer from the TTA ligands to the Eu(III) ion.

Luminescence decay curves of the Eu-complexes were fitted by equation $I(t) = I(0)\exp(-t/\tau)$ using a curve-fitting program, as expected for the presence of only one site of symmetry around Eu(III) ion. The lifetime values (τ) for

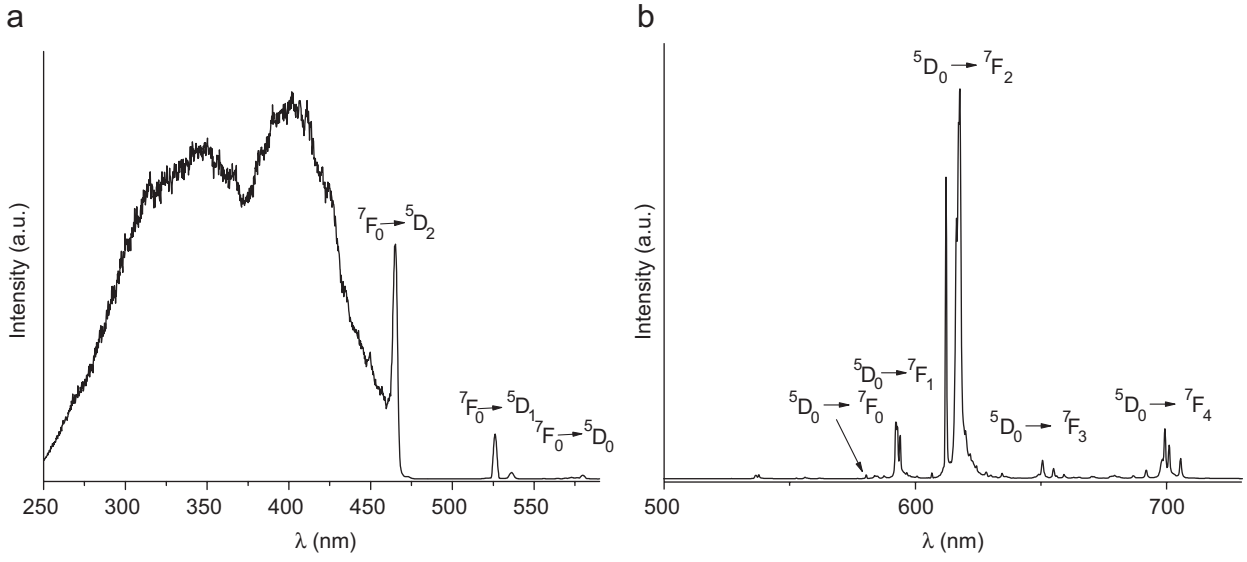


Fig. 3. Photoluminescence spectra of the $[Eu(TTA)_2(NO_3)(TPPO)_2]$ complex in solid state, at 77 K. (a) Excitation spectrum recorded monitoring emission at 615 nm and (b) emission spectrum recorded under excitation at 350 nm.

Table 1
Experimental and theoretical intensity parameters for the $[Eu(TTA)_2(NO_3)(TPPO)_2]$ and $[Eu(TTA)_3(TPPO)_2]$ complexes

Complexes		Ω_2 ($\times 10^{20}$ cm^2)	Ω_4 ($\times 10^{20}$ cm^2)	R_{02}	ΔE (cm^{-1})	A_{rad} (s^{-1})	A_{nrad} (s^{-1})	A_{tot} (s^{-1})	η (%)	Q (%)
$[Eu(TTA)_2(NO_3)(TPPO)_2]$	Experimental	21.8	5.5	0.0016	51	780	446	1225	63	68
	Theoretical	(20.4)	(10.8)	(0.0019)	(199)					(65)
$[Eu(TTA)_3(TPPO)_2]$	Experimental	41.5	9.9	0.0012	172	1444	560	2004	72	73
	Theoretical	(40.0)	(15.3)	(0.0012)	(228)					(73)

bis- and *tris*-TTA complexes are 816 and 500 μs, respectively.

Based on the experimental luminescence data it is possible to determine the Einstein's coefficient of spontaneous emission ($A_{0\to J}$) of the transitions from $^5D_0$ emitting level to ^7F_J levels, arising from Eu(III) ion by the following equation:

$$A_{0\to J} = \frac{\sigma_{0\to 1}}{S_{0\to 1}}\frac{S_{0\to J}}{\sigma_{0\to J}}A_{0\to 1}, \quad (1)$$

where $\sigma_{0\to 1}$ and $\sigma_{0\to J}$ correspond to the energy baricenter of the $^5D_0\to{}^7F_1$ and $^5D_0\to{}^7F_J$ transitions (in cm^{-1}), respectively. In the similar way $S_{0\to 1}$ and $S_{0\to J}$ are the surface of the emission curve corresponding to the $^5D_0\to{}^7F_1$ and $^5D_0\to{}^7F_J$ transitions, respectively [27]. As it can be seen, for Eu(III) complexes the coefficients $A_{0\to J}$ are determined taking the magnetic dipole $^5D_0\to{}^7F_1$ transition as an internal standard since $A_{0\to 1}$ rate is almost insensitive to changes in the chemical environment around the europium ion ($A_{0\to 1}\cong 50\,s^{-1}$). The value of $A_{0\to 1}\cong 50\,s^{-1}$ is taken assuming that the refraction index (n) for the samples is equal to 1.5 [1]. In this work, the radiative contribution is estimated based only on the relative intensities of the $^5D_0\to{}^7F_{0-4}$ transitions owing to the $^5D_0\to{}^7F_{5,6}$ transitions are not observed experimentally.

It is possible to determine the emission quantum efficiency (η) of the $^5D_0$ emitting level the of the Eu^{3+} ion, according to the equation

$$\eta = \frac{A_{rad}}{A_{rad}+A_{nrad}}. \quad (2)$$

The total decay rate $A_{tot} = (1/\tau) = A_{rad} + A_{nrad}$, where A_{rad} ($=\sum_J A_{0\to J}$) and A_{nrad} are the radiative and non-radiative rates, respectively. Thus, based on the experimental lifetime of the $^5D_0$ emitting level (τ) and A_{rad} rate, it was possible to determine the non-radiative rates (A_{nrad}).

The experimental values of the radiative (A_{rad}) and non-radiative (A_{nrad}) rates, and emission quantum efficiency (η) are presented in Table 1. A comparison between the values for Eu(III)-complexes show that the value of A_{rad} for *bis*-TTA complex is twice shorter than that for *tris*-TTA complex, whereas A_{nrad} is only slightly shorter from the former. This behavior reflects a lower emission quantum efficiency (η) for the Eu(III) ion in the *bis*-TTA complex.

Based on the experimental intensity $A_{0\to J}$, the Ω_2 and Ω_4 parameters were determined, according to the following expression:

$$A_{0\to\lambda} = \frac{4e^2\omega^3}{3\hbar c^3(2J+1)}\left[\frac{n(n^2+1)^2}{9}\right]\Omega_\lambda\langle|\alpha J||U^{(\lambda)}||\alpha' J'\rangle^2, \quad (3)$$

where $A_{0\to\lambda}$ are the coefficients of spontaneous emission, χ is the Lorentz local field correction term that is given by $\chi = n(n^2+1)^2/9$ with the refraction index $n = 1.5$ and $\langle{}^7F_\lambda||U^{(\lambda)}||{}^5D_0\rangle^2$ are the squared reduced matrix elements whose values are 0.0032 and 0.0023 to $\lambda = 2$ and 4, respectively [1].

Analysis of the experimental and theoretical intensity parameters (Ω_2 and Ω_4) give a general trend concerning the link between the number of TTA ligand in the first coordination sphere of Eu(III) ion. As a matter of fact, the oxygen atoms that belong to TTA and nitrate ligands differ from their polarizabilities. The delocalization of the π-electrons of the chelate rings in TTA ligands makes their oxygen atoms more polarizable than those from NO_3 ligand. Consequently, when NO_3 is in the place of one TTA group, the chemical environment around the europium ion becomes less polarizable, which is reflected on the values of Ω_2 and Ω_4 parameters.

For experimental determination of luminescence quantum yield (q_x) for the Eu(III) complexes the method developed by Brill and Veenis at Philips Research Laboratories [28–30], as described in Ref. [1], using MgO as reflectance standard, which presents $r \sim 91\%$ was used. The standard phosphor used was sodium salicylate, whose emission spectra are formed by a large broad band peaking around 425 nm, with q value of 60%. The errors in the quantum yield values associated with this technique were estimated within 10%.

The q values of ($[Eu(TTA)_2(NO_3)(TPPO)_2]$ and $[Eu(TTA)_3(TPPO)_2]$) complexes are summarized in Table 1. Considering that the TTA is a ligand that transfers energy efficiently to Eu(III) ion more than nitrate group, the smallest value of q for the *bis*-TTA complex is a consequence of the substitution of the TTA by nitrate ligand in *tris*-TTA complex.

The experimental quantum yields and quantum emission efficiency obtained here for the ($[Eu(TTA)_2(NO_3)(TPPO)_2]$ and $[Eu(TTA)_3(TPPO)_2]$) complexes are similar to the

values found for other Eu–TTA-complexes reported by Malta and co-workers [1], suggesting an operative ligand-to-Eu^{3+} ion energy transfer process.

3.3. Theoretical approach

3.3.1. Theoretical complexes geometries

The geometry of the Eu(III) complexes were obtained using an improved version of the semi-empirical Sparkle model for the calculation of Lanthanide complexes, SMLC [10]. This recent version (called SMLC II) has been applied to lanthanide complexes with a large kind of ligands such as β-diketonates, macrocyclics and heteroaromatics [31].

The predicted geometries of ligand molecules coordinated to the Ln(III) ion (Sparkle model) are calculated with the AM1 Hamiltonian, simulating an essentially electrostatic ligand–metal interaction. In the SMLC II, there is a more confident core–core interaction than that in the previous version [31]. Besides, from the geometry and the electronic states of the ligands, a complete theoretical model may also be applied to calculate the energy transfer processes *antenna*-to-lanthanide ion and the luminescent properties of lanthanide compounds.

Fig. 4 displays the experimental and theoretical structures of the *bis*- and *tris*-TTA complexes. As it can be seen, the theoretical and experimental structures are in agreement, reinforcing the potentiality of the SMLC method in the design of the coordination Eu(III)–TTA complexes. The average unsigned mean error (UME) for each complex was also determined, assuming the distances metal ion–donor atoms (R_{ij}) as those coming from crystal structure data [33]. For $[Eu(TTA)_2(NO_3)(TPPO)_2]$ and $[Eu(TTA)_3(TPPO)_2]$ complexes UME values are 0.0583 and 0.0125, respectively.

3.3.2. Intensity parameter calculation

In order to investigate the ligand–Ln^{3+} interactions and spectroscopic properties for the *bis*-TTA complex, theoretical calculations have been performed. In the present study, the identification and selection of ligand perturber sites (donor atoms) as well as the positional coordinates of these perturber entities were derived from X-ray crystallographic data presented in this work, for $[Eu(TTA)_2(NO_3)(TPPO)_2]$, and reported by Silva for $[Eu(TTA)_3(TPPO)_2]$ complex [22].

The calculations to obtain the Ω_λ intensity parameters ($\lambda = 2$ and 4) were performed according to the following equation [1]:

$$\Omega_\lambda = (2\lambda + 1) \times \sum_{t,p} \frac{|B_{\lambda tp}|^2}{2t+1}, \quad (4)$$

where the quantities $B_{\lambda tp}$ are known as the intensity parameters of individual transitions between Stark levels. As described in the literature, the expression for $B_{\lambda tp}$ contains dependences on the coordination geometry and on the nature of the chemical environment around the Ln^{3+} ion [1]. It is also important to mention that the ligand field parameters used in this work are those given by simple overlap model (SOM) [32,33]. For the calculation, the spherical positional coordinates (r, θ, ϕ) for the oxygen atoms in the first coordination sphere of europium ion in the *bis*- and *tris*-TTA complexes from crystallographic data were used.

The charge factor (g_j) and isotropic polarizability (α_j) to each of the atomic perturber sites were chosen based on the best values of the maximum splitting (ΔE) of the level $^7F_1$ of the Eu(III) ion, intensity parameters $\Omega_{\lambda=2,4}$ and R_{02} better adjusted to their respective experimental values, according to Ref. [22].

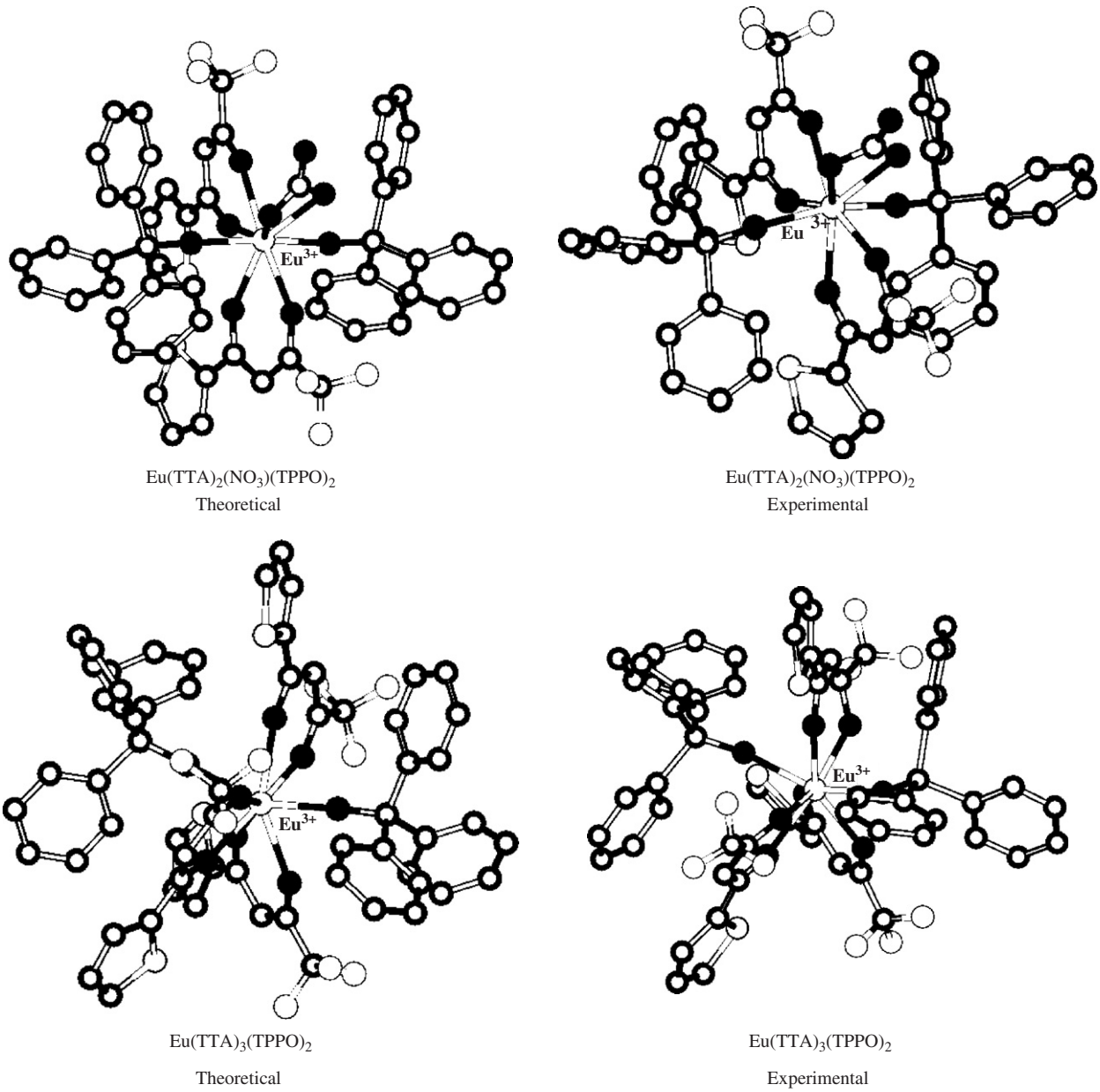
As can be observed in Table 1, in each system good agreement between calculated and observed parameters was achieved, giving evidence that the model calculations reported here is appropriated to describe the chemical environment around Eu^{3+} ion. However, some deficiencies in the intensity parameter calculations may be assigned to the treatment of the ligand properties. For example, in the calculation, the ligand isotropic polarizabilities, for example, were located on atoms only and the ligand polarizability anisotropy was ignored.

The values of g_j and α_j to each of the atomic perturber sites in the *bis*- and *tris*-TTA complexes are the following: for $[Eu(TTA)_2(NO_3)(TPPO)_2]$: $g(TTA) = 1.4$, $g(TPPO) = 1.0$ and $g(NO_3) = 1.0$; $\alpha(TTA) = 4.0$, $\alpha(TPPO) = 4.5$ and $\alpha(NO_3) = 1.0$. For $[Eu(TTA)_3(TPPO)_2]$: $g(TTA) = 0.7$ and $g(TPPO) = 1.0$; $\alpha(TTA) = 4.8$ and $\alpha(TPPO) = 2.8$. Comparisons of the these data reveal the highest α value for oxygen atoms that belong to TTA ligands in the *tris*-TTA complex, indicating a highly polarizable chemical environment around europium ion in the $[Eu(TTA)_3(TPPO)_2]$ complex.

The contributions to forced electric dipole mechanism (Ω_λ^{ED}) and dynamic coupling mechanism (Ω_λ^{DC}) were determined taking α and g values equal to zero, respectively [29,34]. The higher values of Ω_λ^{ED} as compared to those of Ω_λ^{DC} for $[Eu(TTA)_2(NO_3)(TPPO)_2]$ ($\Omega_2^{ED} = 3.2$, $\Omega_2^{DC} = 18.6$, $\Omega_4^{ED} = 0.2$ and $\Omega_4^{DC} = 13.8 \times 10^{-20}\,cm^2$) and for $[Eu(TTA)_3(TPPO)_2]$ ($\Omega_2^{ED} = 1.4$, $\Omega_2^{DC} = 42.5$, $\Omega_4^{ED} = 0.1$ and $\Omega_4^{DC} = 16.4 \times 10^{-20}\,cm^2$) indicate that the dynamic coupling is the dominant mechanism to the radiative transitions in the both complexes. Additionally, since in this mechanism the intensity of the hypersensitive $^5D_0 \rightarrow {}^7F_2$ transitions is related explicitly to the polarizability of the ligands, a comparison between the Ω_2^{ED} values for *bis*-TTA and *tris*-TTA complexes reflects the highest dynamic coupling for the Eu^{3+} center in the $[Eu(TTA)_3(TPPO)_2]$ complex.

3.3.3. Energy transfer rates and quantum yields

The energy transfer rate W_{ET} from TTA-to-Eu(III) ion was investigated according to the theoretical model, presenting the contribution of both dipole–2^λ pole (W_{ET}^{mp}), dipole–dipole (W_{ET}^{dd}) and exchange (W_{ET}^{ex}) mechanisms, as described in Ref. [23].



$Eu(TTA)_2(NO_3)(TPPO)_2$
Theoretical

$Eu(TTA)_2(NO_3)(TPPO)_2$
Experimental

$Eu(TTA)_3(TPPO)_2$
Theoretical

$Eu(TTA)_3(TPPO)_2$
Experimental

Fig. 4. Theoretical and experimental structures $[Eu(TTA)_2(NO_3)(TPPO)_2]$ and $[Eu(TTA)_3(TPPO)_2]$ complexes.

The calculation yields the populations of all states involved in the photophysical process in Eu(III)-complexes, making possible to obtain theoretical quantum yield by the following equation:

$$q = \frac{\eta_e \sum_i A_{ei}}{\eta_a B_a}, \tag{5}$$

where A_{ei} is the radiative transition rate from the emitting level with population η_e to level i, and B_a is the total absorption rate of the absorbing level in a ligand with η_a population.

The main non-radiative energy transfer pathway from TTA-to-Eu(III) ion is also investigated. An analysis of the data in Table 2 reveals that there is no significant difference between the ligand-to-metal energy transfer pathways for *bis*- and *tris*-TTA complexes. Besides, the most probable intramolecular energy transfer processes as operative channels from TTA-to-Eu(III) ion in both complexes is the following: $S_0 \rightarrow S_1 \rightarrow T \rightarrow (^5D_1, ^5D_0) \rightarrow {}^7F_J$.

Of special note is the relatively the remarkable agreement between calculated and experimental values of q for both $Eu(TTA)_2(NO_3)(TPPO)_2]$ and $[Eu(TTA)_3(TPPO)_2]$, suggesting the potentiality of the used model. Moreover, the values of q are close to η ones, indicating that an efficient energy transfer from TTA-to-Eu^{3+} ion in fact occurs.

Table 2
Energy transfer rates from ligand states (singlet and triplet) to europium levels $^{2S+1}L_J$ (Eu^{3+}) in the $[Eu(TTA)_2(NO_3)(TPPO)_2]$ and $[Eu(TTA)_3(TPPO)_2]$ complexes

Energy states	Population	Energy transfer $S_1 \rightarrow {}^{2S+1}L_J$		Energy transfer $T \rightarrow {}^{2S+1}L_J$	
		W_{ET}	W_{RET}	W_{ET}	W_{RET}
$[Eu(TTA)_2(NO_3)(TPPO)_2]$					
S_0	0.924				
S_1	3.21×10^{-8}				
T	1.44×10^{-8}				
$^5D_3$	6.60×10^{-8}	2.12×10^{9}	6.09×10^{6}	4.40×10^{3}	1.02×10^{9}
$^5D_2$	1.47×10^{-6}	4.37×10^{7}	0.00	5.22×10^{1}	1.26×10^{1}
$^5D_1$	6.46×10^{-5}	6.11×10^{8}	0.00	3.05×10^{9}	5.65×10^{3}
$^5D_0$	7.50×10^{-2}	1.23×10^{8}	0.00	1.67×10^{9}	7.55×10^{-1}
$[Eu(TTA)_3(TPPO)_2]$					
S	3.78×10^{-8}				
T	1.81×10^{-8}				
$^5D_3$	1.19×10^{-7}	1.97×10^{9}	1.15×10^{6}	1.90×10^{1}	6.26×10^{8}
$^5D_2$	1.45×10^{-6}	3.53×10^{7}	0.00	1.48	5.06×10^{1}
$^5D_1$	4.51×10^{-5}	4.34×10^{8}	0.00	4.35×10^{9}	1.14×10^{6}
$^5D_0$	0.048	8.02×10^{7}	0.00	3.13×10^{9}	2.01×10^{2}

3.4. Triboluminescent behavior

The $[Gd(TTA)_2(NO_3)(TPPO)_2]$ complex exhibits green light when its crystals are triturated (Fig. 5a). This result confirms that the TL phenomenon in Eu(III)-complexes may occur by indirect excitation of ligands as an intermediate process acting as "antennas", sensitizing the luminescence of Ln(III) ions.

It is important to emphasize that both *bis*-TTA [24] and *tris*-TTA complexes present TL phenomenon exhibit. Fig. 5b shows TL spectra of these complexes recorded at room temperature in the spectral range of 400–750 nm. It is interesting to note that TL spectrum of the $[Eu(TTA)_2(NO_3)(TPPO)_2]$ compound (Fig. 5b) also displays the $^5D_0 \rightarrow {}^7F_1$ transition, which is not shown in the TL spectrum reported in Ref. [24].

According to the experimental evidences presented by Gd(III)-complex, TL for europium complexes may occur by the following processes: (i) break of crystals, (ii) ligand excitation, (iii) energy transfer ligand-to-europium ion and (iv) emission from Eu(III) ion.

Although it is not yet fully clear that the relationship between structural and TL behavior, centric crystals structural disorder can play a role on TL activity [21]. In the present study, it was observed that although the $[Eu(TTA)_3(TPPO)_2]$ complex presents higher PL intensity than $[Eu(TTA)_2(NO_3)(TPPO)_2]$ compound, the former exhibits only very weak TL (Fig. 5b). However, for the *bis*-TTA complex TL phenomenon can be observed even in bright room, giving good evidence that structural behavior dominates the TL properties of the Eu(III)-complexes.

The TL data suggest that the structural properties play an important role in the TL processes and that the presence of a good *antenna* ligand in the Eu(III) complex from the PL point of view does not necessarily indicate that the compound must exhibit high-TL intensity.

4. Conclusion

Theoretical and experimental PL investigations for *bis*- and *tris*-TTA complexes presented the highest α value for oxygen atoms in the *tris*-TTA complex, indicating a highly polarizable chemical environment around Eu(III). In general, it was observed a good agreement between calculated and observed intensity parameters, giving evidence that the model calculations reported here were appropriate to describe the chemical environment around Eu(III) ion. Finally, the comparative TL properties of europium complexes give good evidence that structural behavior dominates the TL activities of these systems.

5. Supplementary data

During the preparation of this paper, we come to know crystallographic data for the $[Eu(TTA)_2(NO_3)(TPPO)_2]$ complex have been recently published by Bukvetskii et al. [24]. However, our crystallographic data for the $[Eu(TTA)_2(NO_3)(TPPO)_2]$ complex already had been deposited with the Cambridge Crystallographic Data Centre as supplementary publication no. CCDC 630702. Copies of the data can be obtained free of charge on application to CCDC, 12 Union Road, Cambridge CB2 1EZ, UK [fax: +44(1223)336-033; e-mail: deposit@ccdc.cam.ac.uk].

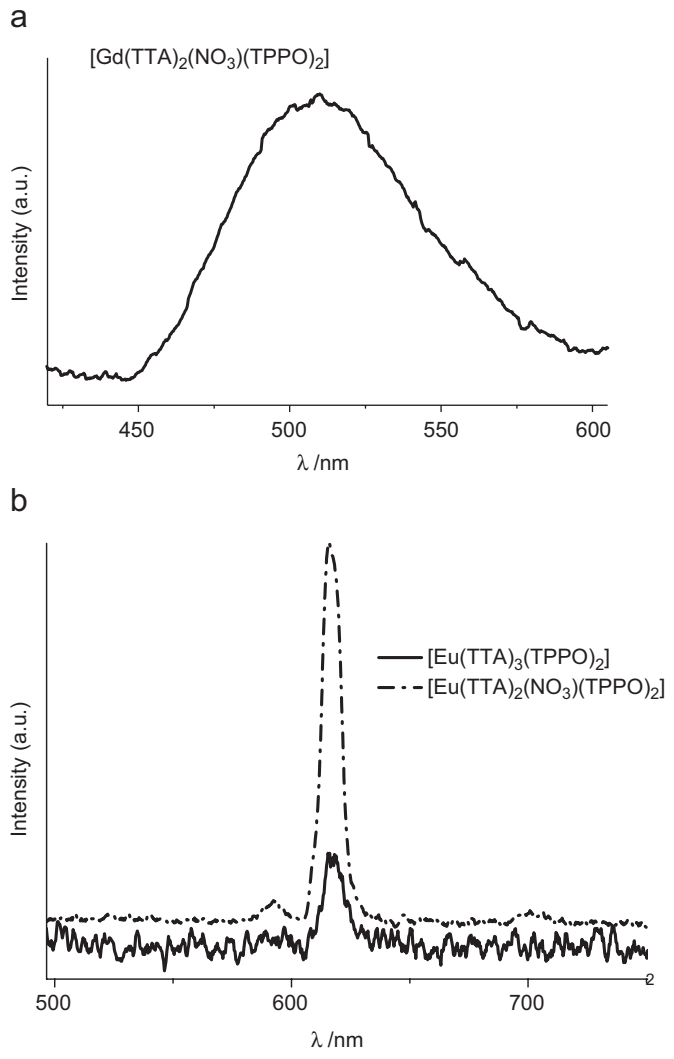


Fig. 5. Triboluminescence spectra recorded for the sample in solid state, at room temperature: (a) TL spectrum of the $[Gd(TTA)_2(NO_3)(TPPO)_2]$ complex and (b) TL spectra of the $[Eu(TTA)_3(TPPO)_2]$ and $[Eu(TTA)_2(NO_3)(TPPO)_2]$ complexes.

Acknowledgments

The authors acknowledge CNPq, RENAMI, FAPESP, and IM^{2}C for financial support. We are grateful to Prof. Mauricio Baptista for the apparatus to record the TL spectra.

References

[1] G.F. de Sá, O.L. Malta, C.D. Donega, A.M. Simas, R.L. Longo, P.A. Santa-Cruz, E.F. Silva, Coord. Chem. Rev. 196 (2000) 165.
[2] I. Hemmila, V.W. Mukkala, Crit. Rev. Clin. Lab. Sci. 38 (2001) 441.
[3] K. Binnemans, Handbook on the Physics and Chemistry of Rare Earths, vol. 35, 2005, p. 107.
[4] R. Reyes, M. Cremona, E.E.S. Teotonio, H.F. Brito, O.L. Malta, Chem. Phys. Lett. 396 (2004) 54.
[5] J. Kido, Y. Okamoto, Chem. Rev. 102 (2002) 2357.
[6] Y. Zhang, H.H. Shi, Y. Ke, Y. Cao, J. Lumin. 124 (2007) 51.
[7] A.A. Petushkov, S.M. Shilov, M.V. Puzyk, V.N. Pak, Technol. Phys. Lett. 32 (2006) 399.
[8] S. Gago, J.A. Fernandes, J.P. Rainho, R.A.S. Ferreira, M. Pillinger, A.A. Valente, T.M. Santos, L.D. Carlos, P.J.A. Ribeiro-Claro, I.S. Gonçalves, Chem. Mater. 17 (2005) 5077.
[9] P. Lenaerts, E. Ryckebosch, K. Driesen, R. Van Deun, P. Nockemann, C. Groller-Walrand, K. Binnemans, J. Lumin. 114 (2005) 77.
[10] A.V.M. Andrade, N.B. Costa, A.M. Simas, G.F. de Sá, Chem. Phys. Lett. 227 (1994) 349.
[11] A.V.M. Andrade, N.B. Costa, A.M. Simas, G.F. de Sá, J. Alloys Compd. 225 (1995) 55.
[12] H.J. Batista, A.V.M. Andrade, R.L. Longo, A.M. Simas, G.F. de Sá, N.K. Ito, L.C. Thompson, Inorg. Chem. 37 (1998) 3542.
[13] G.D. Qian, M.Q.J. Wang, Am. Ceram. Soc. 83 (2000) 703.
[14] C.G. Gameiro, C.A. Achete, R.A. Simão, E.F. da Silva, P.A. Santa-Cruz, J. Alloys Compd. 344 (2002) 385.
[15] P. Nockemann, E. Beurer, K. Driesen, R.V. Deun, K.V. Hecke, L.V. Meervelt, K. Binnemans, Chem. Commun. 34 (2005) 4354.
[16] P.P. Lima, R.A.F. Sá, R.O. Freire, F.A.A. Paz, L. Fu, S. Alves Jr., L.D. Carlos, O.L. Malta, Chem. Phys. Chem. 7 (2006) 735.
[17] J.-C.G. Bünzli, Lanthanide Probes in Life Chemical Earth Sciences, in: J.-C.G. Bünzli, G.R. Chopin (Eds.), Elsevier, New York, 1989.
[18] Y.J. Fu, T.K.S. Wong, Y.K. Yan, X. Hu, J. Alloys Compd. 258 (2003) 235.
[19] F.A. Cotton, L.M. Daniels, P.L. Huang, Inorg. Chem. Commun. 4 (2001) 319.
[20] F.A. Cotton, P.L. Huang, Inorg. Chem. Acta 346 (2003) 223.
[21] L.M. Sweeting, J. Am. Chem. Soc. 109 (1987) 2652.
[22] C.F.B. Silva, Ph.D. Thesis, University of São Paulo, 2002.
[23] E.E.S. Teotonio, H.F. Brito, M.C.F.C. Felinto, L.C. Thompson, V.G. Young, O.L. Malta, J. Mol. Struct. 751 (2005) 85.
[24] B.V. Bukvetskii, A.G. Mirochnik, P.A. Zhikhareva, V.E. Karasev, J. Struct. Chem. 47 (2006) 575.
[25] K. Nakamoto, Infrared and Raman Spectra of Inorganic and Coordination Compounds, third ed., Wiley, New York, 1978.
[26] Y. Fukuda, A. Nakao, K. Hayashi, J. Chem. Soc. Dalton Trans. 4 (2001) 527.
[27] W.M. Faustino, S.A. Junior, L.C. Thompson, G.F. de Sá, O.L. Malta, A.M. Simas, Int. J. Quantum Chem. 103 (2005) 572.
[28] A. Brill, W.J. Veenis, J. Res. Nat. Bureau Stand. 80A (1976) 401.
[29] A. Brill, W.J. Veenis, J. Electrochem. Soc. 123 (1976) 396.
[30] A. Brill, W.J. Veenis, Philips J. Res. 33 (1978) 124.
[31] G.B. Rocha, R.O. Freire, N.B. da Costa Jr., G.F. de Sá, A.M. Simas, Inorg. Chem. 43 (2004) 2346.
[32] O.L. Malta, Chem. Phys. Lett. 88 (1982) 353.
[33] O.L. Malta, M.A. Couto dos Santos, L.C. Thompson, N.K. Ito, J. Lumin. 69 (1996) 77.
[34] O.L. Malta, H.F. Brito, J.F.S. Menezes, F.R.G. Silva, S.A. Farias, A.V.M. Andrade, J. Lumin. 75 (1997) 255.